AUTHOR QUERY FORM

Journal: NUMA

Article Number: 46362

Please e-mail or fax your responses and any corrections to:

E-mail: corrections.esch@elsevier.sps.co.in

Fax: +31 2048 52799

Dear Author,

Please check your proof carefully and mark all corrections at the appropriate place in the proof (e.g., by using on-screen annotation in the PDF file) or compile them in a separate list. Note: if you opt to annotate the file with software other than Adobe Reader then please also highlight the appropriate place in the PDF file. To ensure fast publication of your paper please return your corrections within 48 hours.

For correction or revision of any artwork, please consult http://www.elsevier.com/artworkinstructions.

Any queries or remarks that have arisen during the processing of your manuscript are listed below and highlighted by flags in the proof. Click on the 'Q' link to go to the location in the proof.

Location in article	Query / Remark: click on the Q link to go Please insert your reply or correction at the corresponding line in the proof
Q1	Please confirm that given names and surnames have been identified correctly.
Q2	Please check the identification of corresponding author and details.
Q3	Please note that Figs. 1–4 will appear in B/W in print and color in the web version. Based on this, please approve the footnote 1 which explains this.

Thank you for your assistance.

Journal of Nuclear Materials xxx (2012) xxx–xxx

Contents lists available at SciVerse ScienceDirect

Journal of Nuclear Materials

journal homepage: www.elsevier.com/locate/jnucmat

Phonon spectrum, thermal expansion and heat capacity of UO_2 from first-principles

Younsuk Yun[a,b,*], Dominik Legut[c,d], Peter M. Oppeneer[a]

[a] Department of Physics and Astronomy, Uppsala University, Box 516, SE-751 20 Uppsala, Sweden
[b] Laboratory of Reactor Physics and Systems Behaviour, Paul Scherrer Institut, CH-5232 Villigen PSI, Switzerland
[c] Nanotechnology Centre, VSB-Technical University of Ostrava, 17. listopadu 15, CZ-708 33 Ostrava, Czech Republic
[d] Atomistic Modeling and Design of Materials, University of Leoben, Leoben, Austria

ARTICLE INFO

Article history:
Received 6 December 2011
Accepted 10 March 2012
Available online xxxx

ABSTRACT

We report first-principles calculations of the phonon dispersion spectrum, thermal expansion, and heat capacity of uranium dioxide. The so-called direct method, based on the quasiharmonic approximation, is used to calculate the phonon frequencies within a density functional framework for the electronic structure. The phonon dispersions calculated at the theoretical equilibrium volume agree well with experimental dispersions. The computed phonon density of states (DOSs) compare reasonably well with measured data, as do also the calculated frequencies of the Raman and infrared active modes including the LO/TO splitting. To study the pressure dependence of the phonon frequencies we calculate phonon dispersions for several lattice constants. Our computed phonon spectra demonstrate the opening of a gap between the optical and acoustic modes induced by pressure. Taking into account the phonon contribution to the total free energy of UO_2 its thermal expansion coefficient and heat capacity have been computed from first-principles. Both quantities are in good agreement with available experimental data for temperatures up to about 500 K.

1. Introduction

Over the last few decades UO_2 has been one of most widely studied actinide oxides due to its technological importance as standard fuel material used in nuclear reactors. There exists currently considerable interest in understanding the behavior of nuclear fuel in reactors which is a complex phenomenon, influenced by a large number of materials' properties, such as thermomechanical strength, chemical stability, microstructure, and defects. Especially, knowledge of the fuel's thermodynamic properties, such as specific heat, thermal expansion, and thermal conductivity, is essential to evaluate the fuel's performance in nuclear reactors [1–5]. These thermodynamic quantities are directly related to the lattice dynamics of the fuel material [6–9].

Dolling et al. [10] were the first to measure phonon dispersion curves of UO_2, using the inelastic neutron scattering technique in 1965; their seminal article has become the standard reference for uranium dioxide's phonon spectrum. Later the vibrational properties of UO_2 were investigated in detail by Schoenes [11], using infrared and Raman spectroscopic techniques. A good agreement with phonon frequencies obtained from inelastic neutron scattering was observed [11]. More recently, Livneh and Sterer [12] studied the influence of pressure on the Raman scattering in UO_2 and Livneh [13] demonstrated the resonant coupling between longitudinal optical (LO) phonons and U^{4+} crystal field excitations in a Raman spectroscopic investigation. A theoretical investigation of the phonon spectra of UO_2 was reported recently by Yin and Savrasov [14] who employed a combination of a density-functional-theory (DFT) based technique and a many-body approach. According to their results, the low thermal conductivity of UO_2 stems from the large anharmonicity of the LO modes resulting in no contribution from these modes in the heat transfer. Goel et al. [15,16] investigated the phonon properties of UO_2 using an empirical interatomic potential based on the shell model and observed that the calculated thermodynamic properties including the specific heat are in good agreement with available experimental data. Devey [17] employed recently the generalized gradient approximation with [SC1] Hubbard U (GGA + U) to compute the main phonon mode frequencies at the Brillouin zone center which were in reasonable agreement with experimental data. Very recently, Sanati et al. [18] used the GGA and GGA + U approaches to investigate phonon density of states and elastic and thermal constants, which were found to be in reasonably good agreement with experimental data. In spite of the already performed studies, further investigations are still needed. Especially, the full dispersions of the phonons in reciprocal space have not yet been considered. Also, important quantities such as the thermal expansion coefficient and heat capacity at constant pressure are directly related to the

* Corresponding author at: Laboratory of Reactor Physics and Systems Behaviour, Paul Scherrer Institut, CH-5232 Villigen PSI, Switzerland.
E-mail address: younsuk.yun@psi.ch (Y. Yun).

0022-3115/$ - see front matter © 2012 Published by Elsevier B.V.
http://dx.doi.org/10.1016/j.jnucmat.2012.03.017

volume-dependent lattice vibrations, but there has been a lack of studies of these quantities using the phonon spectra calculated from first-principles techniques.

The objective of this study is to contribute to a detailed understanding of the lattice vibrations of UO_2. Using the first-principles approach, based on the DFT we have calculated phonon dispersion curves and phonon density of states of UO_2. The calculated phonon properties are compared with the available experimental data from inelastic neutron scattering and Raman spectroscopy along with a detailed discussion. Furthermore, several thermodynamic properties have been computed taking the influence of lattice vibrations into account. Here, we report the lattice contribution to the heat capacity as function of temperature as well as temperature and volume (in the quasiharmonic approximation). The dependence of the total free energy on the lattice constant of UO_2 as a function of temperature has [SC2] been calculated, from which we derive the thermal expansion coefficient. The thermal expansion coefficient as well as lattice heat capacity compare favorably to available experimental data up to 500 K, which is the temperature range in which the influence of anharmonicity can be neglected.

2. Computational methodology

The electronic structure of UO_2 has been discussed in the past years [19–29]. DFT calculations within the generalized gradient approximation (GGA) underestimate the influence of the strong on-site Coulomb repulsion between the 5*f* electrons. An improved 5*f* electronic structure description can be obtained with the GGA + *U* approach, in which a [SC3] on-site Coulomb repulsion term is added; this approach correctly gives the electronic band gap of UO_2 [19,23,30–32]. While the GGA + *U* approach would appear preferable for description of UO_2's electronic structure, we encountered specific problems when using this method. Some of the phonon branches became imaginary away from the zone center. This artifact might be related to the occupation matrix of 5*f* states that would require an additional stabilizing constraint in the GGA + *U* method [25,26]. Apart from the imaginary phonon problem, a recently published [18] phonon spectrum of UO_2 using the GGA + *U* method shows a notable difference with experiments for high-frequency branches, in particular, significantly [SC4] lower-frequency longitudinal optical modes near the Γ-point. Using conversely the spin-polarized GGA approach, we found that such difficulties with imaginary phonon frequencies did not occur. The phonon dispersion spectrum presented below is hence computed with the GGA exchange–correlation for antiferromagnetically ordered UO_2 and is found to be in good agreement with experiment [10].

[SC5-1,3] The application of the GGA methodology to describe thermal properties of oxides has been considered previously. Derzsi et al. [34] reported that the heat capacities of Fe_2SiO_4 and Mg_2SiO_4 using the GGA method are in very good agreement with experiments. In the work of Sanati et al. [18], the phonon DOS of UO_2 obtained from the GGA method was compared to that obtained with the GGA + *U* approach. When the GGA approach is used, the main difference found is that the highest-frequency phonon DOS is slightly shifted to lower frequencies. The integrated phonon DOS is however very similar between the GGA and GGA + *U* calculations (the GGA calculation gives a 1.73% larger value than the GGA + *U*). It can thus be expected that the phonon contribution to the thermodynamic quantities will not significantly differ between the GGA and GGA + *U* calculations.

Here, we have determined the phonon dispersion curves and density of states (DOSs) in the quasiharmonic approximation using the direct method [35,36]. By displacing one atom in a supercell (of 96 atoms) from its equilibrium position, non-vanishing Hellmann–Feynman forces were generated. Due to the high symmetry of the face-centered cubic (fcc) lattice of UO_2, only one atom for uranium (U) and for oxygen (O) [SC6] needed to be displaced. The actual shift of the atoms in the supercell had an amplitude of 0.03 Å and was taken along the [0 0 1] direction only, on account of the cubic symmetry of UO_2. In the calculation of the resulting forces we employed the projector augmented wave (PAW) pseudopotential approach within the Vienna Ab-initio Simulation Package [SC7] (VASP version 4.6) [37,38]. The PHONON code [35,36] has been used to extract the force constant matrix from the Hellmann–Feynman forces and to subsequently calculate the phonon dispersion curves and DOS.

For the thermodynamic quantities we consider the total free energy of UO_2, including the phonon contribution,

$$F(\epsilon,T) = U(\epsilon) + F^{phon}(\epsilon,T) + F^{el}(\epsilon,T), \tag{1}$$

where $F(\epsilon,T)$ is the Helmholtz free energy at a given strain ϵ. The phonon free energy contribution F^{phon} is expressed as

$$F^{phon}(\epsilon,T) = \int_0^\infty d\omega\, g(\omega,\epsilon)[\hbar\omega/2 + k_B T\ \ln(1 - e^{-\hbar\omega/k_B T})], \tag{2}$$

where $g(\omega,\epsilon)$ is the phonon DOS, computed as mentioned above. We note that the free electronic energy, $F^{el}(\epsilon,T)$, is not considered in the present study, because the thermal electronic contribution is known to be negligible in the temperature range up to 1000 K, which is the range of interest in this work [41,42]. The static lattice energy $U(\epsilon)$ appearing in Eq. (1) can be expressed as

$$U(\epsilon) = U_0 + V\sum_{ij} C_{ij}\epsilon_i\epsilon_j, \tag{3}$$

where U_0 is the static lattice energy at zero strain, C_{ij} are the elastic constants, and V is the equilibrium volume at $T = 0$ K. The static lattice energies have also been calculated using the VASP code [37,38].

[SC7][Rev2-C1] In our calculations we have used a $2 \times 2 \times 2$ supercell containing 96 atoms. The supercell size was chosen such that interactions between equivalent ions in periodic images become negligible. The $2 \times 2 \times 2$ supercell has been successfully used in phonon calculations and provided results in good agreement with measurements [39,33,40]. Also, it has been reported that using larger supercells did not lead to significant differences from results with the $2 \times 2 \times 2$ supercell [40]. The total energies of the supercell were calculated by integration over a $4 \times 4 \times 4$ *k*-point mesh in the Brillouin zone (BZ). A high kinetic energy cut-off of 600 eV was used in the calculations, the energy criterion for convergence was set to 10^{-7} eV, and the forces acting on each ion were converged until less than 0.01 eV/Å. The Perdew–Wang parametrization [43] of the GGA functional was used for the exchange correlation interaction.

Once the phonon DOS has been calculated, the thermal expansion of UO_2 can be evaluated straightforwardly. First, the phonon DOS with static lattice energy is calculated for several volumes around the $T = 0$ K equilibrium volume. Subsequently, the total free energies are calculated for these different volumes at constant temperature using Eqs. (1)–(3). After the free energy has been calculated its minimum gives the corresponding equilibrium volume at the considered temperature. By repeating the process for different temperatures, the thermal expansion coefficient α defined by

$$\alpha(T) \equiv \frac{1}{a}\frac{da}{dT} = \frac{1}{3V}\frac{dV}{dT}, \tag{4}$$

is obtained; here a is the lattice constant.

A further thermodynamic quantity, the lattice contribution to the specific heat can be derived from $\frac{\delta F(V,T)}{\delta T}$ at a fixed temperature in the quasiharmonic approximation.

3. Results and discussion

3.1. Ground-state properties of UO_2

UO_2 crystallizes in the cubic fluorite structure (CaF_2) belonging to the $Fm\bar{3}m$ space group (No. 225) and there are three atoms per primitive unit cell with one U atom (Wyckoff position 4*a*) and two inequivalent O atoms (Wyckoff positions 8*c*). Therefore, there are generally nine phonon branches. Before turning to the description and analysis of the calculated lattice dynamics let us briefly consider the ground-state properties of UO_2. As mentioned above the employed DFT framework is that of the spin-polarized GGA where the magnetic moments at the U ions are alternating along the [0 0 1] direction, so-called 1-k antiferromagnetic ordering. The calculated equilibrium lattice constant *a* and bulk modulus *B*, which we have obtained by a Birch–Murnaghan 3rd order fit [44], are presented in Table 1, where these are compared to experimental lattice properties [45–48]. Our calculated equilibrium volume as well as the bulk modulus compare reasonably well with the experimental data and with results from molecular dynamics simulations [7,8]. Compared to the experimental lattice constant the lattice constant computed here is 1.2% smaller. This can be attributed to a too strong binding of the 5*f* orbitals which become too [SC8] delocalized in the spin-polarized-GGA approach. In the GGA + *U* approach the 5*f* orbitals are more localized and their contribution to the bonding reduced [22,19,25], which leads to a theoretical lattice parameter which is larger than the experimental one [28].

3.2. Phonon spectrum of UO_2

Fig. 1 shows the measured and first-principles calculated phonon dispersion curves of UO_2 along high-symmetry points of the fcc BZ. The black lines are the calculated phonon dispersions obtained for the different lattice parameters, the blue open symbols are the experimentally measured data from inelastic neutron scattering [10], and red closed symbols are data from Raman scattering [13]. Note that *M* denotes the additional point (1,1,0) that was included by Dolling et al. [10], but that is outside of the first BZ. The calculated phonon dispersions along the high-symmetry lines *X*–*W*–*Γ* have been added to illustrate the whole dispersion of phonon states in the BZ. The three branches in the low frequency region are the transverse acoustic (TA) and longitudinal acoustic (LA) modes that belong to vibrations of the U atom with its relatively heavy mass. The other branches are optical modes with higher frequencies that are mainly associated with lattice vibrations of O atoms and can be labeled as TO1, LO1 and TO2 and LO2, respectively (see Fig. 1), as there are two inequivalent O atoms in the unit cell. The three panels in Fig. 1 illustrate the volume dependence of the phonon frequencies, which have been calculated at three different lattice constants, the experimental one, $a = 5.47$ Å, the optimized theoretical one, $a = 5.406$ Å, and $a = 5.33$ Å, a selected smaller lattice constant.

[SC9] Close to the *Γ* point the agreement between the calculated and measured phonon frequencies is very good. A first discrepancy between measured and computed dispersions is observed along the *M*–*Γ* high-symmetry direction. Our calculations predict three acoustic branches whereas in experiment there are two branches. It could be that a splitting of the low-lying TA branch near the *M* point could not be sufficiently resolved in the experiment. This might be related to the inelastic neutron scattering technique, which might be affected by the size of samples and as well as a relatively low neutron flux (see e.g., Refs. [49,50]). Also, as mentioned by Dolling et al. the frequency measurements of the phonons with the neutron technique might be impeded in the zone boundary regions. The LO and TO branches agree reasonably well with experiment, in particular for the optimized theoretical lattice parameter. There are some discrepancies in the positions of the branches at the zone boundary *X* and at the *M* point. One of the TO1 branches turning up from the *Γ* point to the *M* point has not been detected in the experiment. Along *Γ*–*L* the agreement is quite good. The top-most (LO2) branch deviates most between calculation and the experiment. This high-lying branch has the largest experimental uncertainty. Nonetheless, the first-principles calculated branch has more dispersion than the corresponding one in the measurements, and, except for the zone center, it falls outside of the experimental error bar.

The phonon frequencies calculated at $a = 5.406$ Å and $a = 5.47$ Å are very similar to each other and agree reasonably well with the measurement data. A notable difference between the two sets of dispersion curves appears however in the frequency gap at the zone boundaries of *M* and *X*. When the lattice constant decreases with pressure from $a = 5.47$ Å to $a = 5.33$ Å a pressure-induced phonon softening occurs. The frequency gap between LA and TO1 modes at the zone boundary *X* point and at the *M* point is increased as the pressure increases. At $a = 5.47$ Å the LA and TO1 modes almost approach each other, whereas at $a = 5.406$ Å, a gap is predicted to exist between the LA and TO1 modes. A small or vanishing gap between these modes is in accordance with the

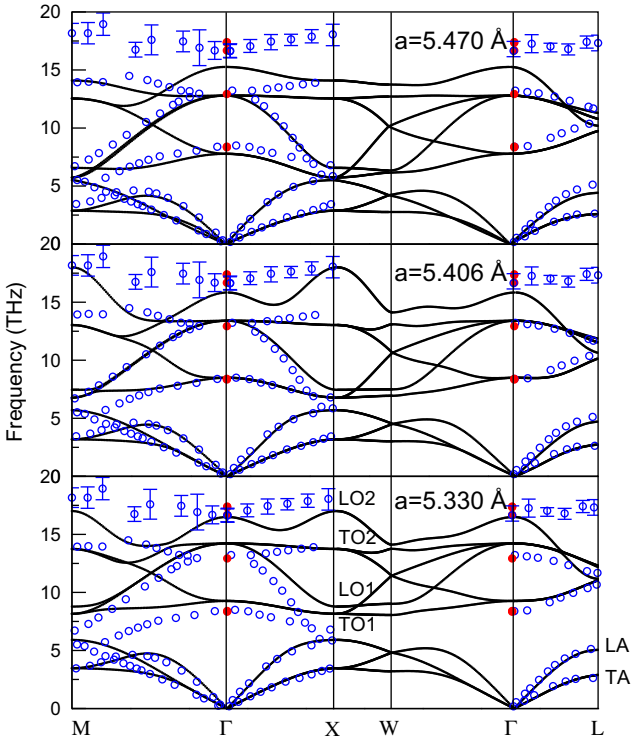

Fig. 1. Calculated (full lines) and measured phonon dispersion curves (open symbols, from Ref. [10]) along high-symmetry directions in the fcc Brillouin zone. The measured Raman and infrared modes (Ref. [13]) at the *Γ* point are depicted by solid (red) circles. The notation of the special points is *M*: (1,1,0), *Γ*: (0,0,0), *X*: (1,0,0), *W*: $(1,\frac{1}{2},0)$, and *L*: $(\frac{1}{2},\frac{1}{2},\frac{1}{2})$.

Table 1
Calculated equilibrium lattice constant *a* (in Å) and bulk modulus *B* (in GPa) of UO_2. Theoretical values obtained in this work are compared to values from molecular dynamics simulations [7] (MD), as well as to experimental data [45–48] (exp.).

	a (Å)	*B* (GPa)
This work	5.406	184
MD (300 K)	5.472 [7]	182 [7]
Exp. (300 K)	5.47 [45,46]	192 [47], 198 [45], 207 [46]

measurement. We also note that with increased lattice constant the negative slope of the LO1 branch is remarkably increased along the Γ–X symmetry line. This finding suggests that the propagation of the LO1 phonon is significantly restrained as the lattice constant increases.

In Fig. 1 [SC11] we furthermore depicted the frequencies obtained by Raman and infrared measurements at the Γ point, which are indicated with red solid circles [11,13]. Using group theory analysis these active Raman and infrared modes can be decomposed into irreducible representations of the (O_h^5) space group, as $1T_{2g} + 2T_{1u}$. The U atom contributes only to the infrared active mode (T_{1u}), whereas the O atom contributes to both, the infrared and Raman mode, T_{1u} and T_{2g}, respectively. Both these modes are triply degenerate. The frequencies of these modes are summarized in Table 2, together with results from MD simulations [16] and experimental results [10,11,13]. To account for the LO/TO splitting the Lyddane–Sachs–Teller [51] relation was used on the basis of effective charges. These were chosen to be 3 for the uranium atom and −1.5 for oxygen. These values are consistent with values used in the literature [15]. The macroscopic electric field in UO_2 splits the infrared-active optical modes into TO and LO components. Frequencies of TO modes are calculated in a straightforward manner within the direct method but the LO modes can only be obtained via introduction of a non-analytical term [52] into the dynamical matrix. In general, this term depends on the Born effective charge tensor and the electronic part of the dielectric function (high-frequency dielectric constant). [Rev2-C2] To account for the non-analytical contribution, the dynamical matrix is written as the sum of force constants derived from Hellmann–Feynman forces and a non-analytical term. Assuming that the effective charge tensor can be approximated by a point charge which is given by the Born effective charge, the frequencies of the LO modes at the Γ point are calculated using the point charges. Details regarding this procedure can be found elsewhere, see e.g. [54].

The agreement of the computed Raman optical mode as well as the infrared TO mode with available experimental data is quite good, see Table 2. The calculated frequency of the infrared LO mode is somewhat smaller than the experimental results, indicating that the effective charge and dielectric constant taken from literature do not fully account for the correct $\frac{\varepsilon_0}{\varepsilon_\infty} = \frac{\omega_{LO}^2}{\omega_{TO}^2}$. In addition there is a spread of ca. 0.7 THz in the measured values of the LO infrared mode frequencies [53,11]. This is, however, not sufficient to account for the underestimation of the experimental values by about 2 THz that is observed for $a = 5.470$ Å (upper panel of Fig. 1). Using the calculated theoretical volume (middle panel of Fig. 1) this deviation is reduced by 25%. A similar error of ca. 1.5 THz for the first-principles calculated infrared frequencies of another insulating compound, $CsNiF_3$, was reported in a recent study [55].

Fig. 2 shows the calculated and experimental phonon DOS, where the latter was obtained by a fit to the shell-model using the measured phonon dispersions [10]. The blue, red, and green lines with square, triangle, and diamond symbols indicate the phonon DOS computed for $a = 5.330$ Å, 5.406 Å, and 5.470 Å, respectively. The experimental data [10] ($a \approx 5.47$ Å, $T = 296$ K) are plotted with the black line. The U contribution to the calculated phonon DOSs gives rise to a higher intensity and narrower peak widths in the lower frequency region. The more broadened DOS with lower intensity that occurs in the higher frequency region is mainly derived from the oxygen atoms. A notable difference between the phonon DOS at the three lattice parameters is the size and position of the phonon gap occurring for frequencies of about $6 - 7$ THz. For the experimental lattice parameter $a = 5.47$ Å the computed gap practically closes. The experimental phonon DOS spectrum at this lattice parameter shows a minimum at about 6 THz, in reasonable agreement, considering some experimental broadening. We note that the trend of decreasing gap with larger lattice constant continues, leading to a closing of the gap computed for larger lattice constants (not shown). Overall, the computed phonons DOS of both the theoretical equilibrium ($a = 5.406$ Å) and the experimental lattice parameter are in good accordance with the measured spectrum. The phonon DOS of the theoretical lattice parameter agrees best with the experimental data at higher frequencies (7–13 THz), where the peaks coincide with the measured ones. As mentioned earlier, the LO2 mode lies both lower in the computed spectra and is more dispersive than in the measurements. We note in this respect that recent GGA + U calculations [18] provided a sharper DOS peak at 17 THz, due to the presence of a flatter LO2 dispersion near the zone boundaries. However, the LO branch falls substantially below the TO branch at the zone center, resulting in that the computed LO2 branch lies much deeper than in the experiment, at 10 THz (*vs.* 17 THz in experiment).

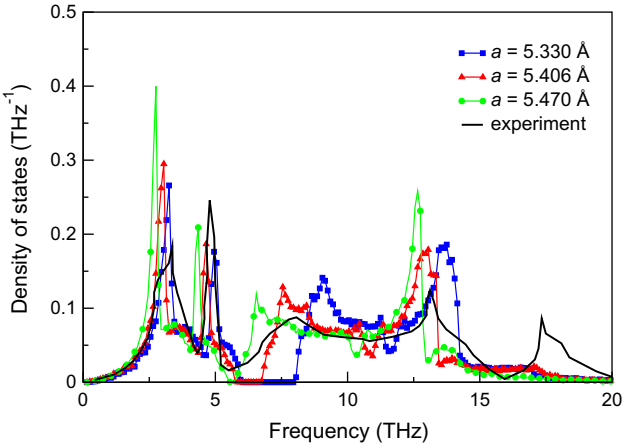

Fig. 2. The theoretical phonon density of states (DOSs) of UO_2 computed for three lattice constants $a = 5.330$, 5.406, and 5.470 Å, compared to the experimental DOS (for $a \approx 5.470$ Å, at $T = 296$ K) that was obtained by a fit to a shell-model using the measured phonon dispersions [10].

Table 2
The frequencies of the Raman (T_{2g}) and infra-red (T_{1u}) vibrational modes of UO_2 at the Γ-point. Theoretical results (this work) are given for three lattice constants a and compared to frequencies obtained from molecular dynamics simulation [16] (MD) as well as experimental (exp.) frequencies (given in THz).

Mode	This work			MD [16]	Exp.
a (Å)	5.33	5.406	5.47	5.47	5.47
T_{1u}(TO)	9.27	8.49	7.78	7.62	8.34 [53], 8.4 [11] 8.52 [10]
T_{1u}(LO)	16.5	15.82	15.26	17.28	16.68 [53], 16.7 [10] 17.34 [11], 17.4 [13]
T_{2g}	14.22	13.4	12.80	14.04	12.93 [53], 13.42 [10]

3.3. Thermal expansion of UO_2

The calculated phonon DOS enables us to evaluate some thermodynamic quantities which depend on the lattice vibrations. We start with the thermal expansion. The phonon contribution to the total free energy of UO_2 increases with increasing temperature and hence becomes progressively responsible for changes of the lattice parameters. To compute the thermal expansion of UO_2 we have first computed the total free energy, including the phonon contribution, for various lattice parameters, from which we computed the temperature-dependent lattice constant. Fig. 3 (bottom) shows the calculated variation of the lattice constant with temper-

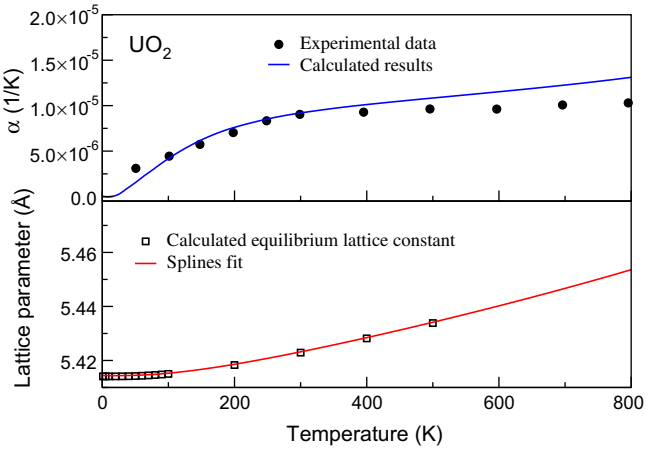

Fig. 3. Top: Calculated and experimental thermal expansion coefficient $\alpha(T)$ of UO_2. The experimental data are those of Taylor [56]. Bottom: Computed temperature-dependent lattice parameter of UO_2 (open squares) and spline fit function.

ature. The red[1] curve gives the spline interpolation of the calculated lattice constants, shown by the symbols. The thermal expansion coefficient $\alpha(T) = a^{-1}da/dT$ was subsequently evaluated by differentiating the spline fit. The upper panel of Fig. 3 shows the calculated thermal expansion coefficient, which is in good agreement with experimental data [56] up to 500 K. The deviation between the calculated and measured data slightly increases above 500 K and becomes significant at around 1000 K. This might be due to an increased electronic contribution to the thermal expansion. At very low temperatures, in the region between 0 and 50 K, a deviation is also observed between the calculated and measured data. The origin of this deviation is not unambiguously clear. We note however that UO_2 undergoes a magnetic phase transition at 31 K (see Ref. [57]), which may add an additional influence on the lattice parameter.

3.4. Thermodynamic properties of UO_2

Next, we employ the Helmholtz free energy to compute the lattice heat capacity at constant volume (C_V) and at constant pressure (C_P). Fig. 4 shows theoretical results for C_V, computed with the harmonic approximation, and C_P, computed with the quasiharmonic approximation, as well as experimental results [58,60] for C_P up to 1000 K. First the lattice contribution to the specific heat C_V was computed as a function of temperature for the equilibrium lattice constant, $a = 5.406$ Å. Subsequently, the specific heat at constant pressure was derived according to

$$C_P = C_V + 9\alpha^2 B a^3 T, \tag{5}$$

where $\alpha(T)$, a, and B are the calculated linear thermal expansion coefficient, the equilibrium lattice constant, and the bulk modulus (see e.g., [61]). Fig. 4 illustrates that there is a very good agreement between the computed heat capacity C_P and the experimental data [58–60]. Note that the sharp anomaly in the experimental data at $T \approx 31$ K is due to the aforementioned magnetic phase transition [57], [SC13]. The effect of which is not included in the calculations. Clearly, the specific heat at constant pressure is in much better agreement with the experimental data at higher temperatures than C_V, which is mainly due to the thermal expansion of UO_2. Conversely, evaluating C_P for the theoretical equilibrium lattice constant or for the experimental lattice constant $a = 5.47$ Å only gives very minor differences. The computed C_P curves fall somewhat below the experimental C_P data for temperatures in the range of 400–1000 K. The uranium atoms in UO_2 are in the paramagnetic state at higher temperatures [11,48]. Therefore, the remaining difference between experimental and computed data above $T > 400$ K could be due to the magnetic entropy contribution to the specific heat or, alternatively, it could be due to the anharmonic effects. The magnetic entropy contribution to the specific heat was investigated for $T = 200$–300 K in Refs. [57,59]. At higher temperatures it saturates to approximately $S = R\ln 3$, corroborating a triplet state on the uranium atoms. It provides a relatively small magnetic entropy contribution that would lead to a small increase of the computed C_P data (by about 3 J mol^{-1} K^{-1}).

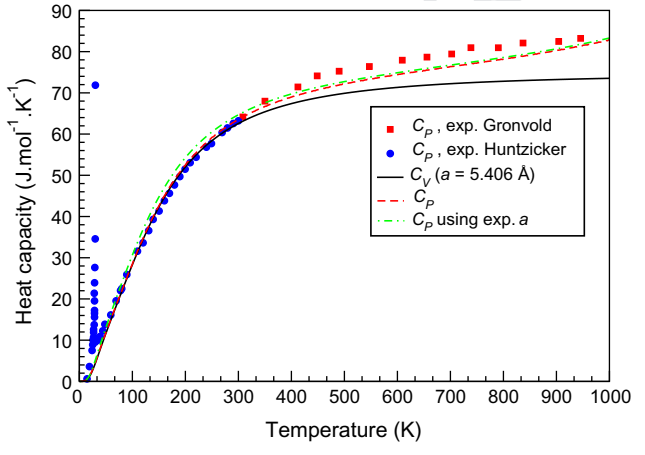

Fig. 4. The lattice contribution to the heat capacity of UO_2 at constant volume, C_V, computed within the harmonic approximation (full curve), and a constant pressure, C_P, computed with the quasiharmonic approximation (dashed lines; for $a = 5.406$ Å and the experimental $a = 5.47$ Å). The experimental data for lower and higher temperatures, full circles and full squares, are taken from Huntzicker and Westrum (Ref. [58]) and Grønvold et al. (Ref. [59]), respectively.

4. Conclusions

We have performed first-principles calculations using the spin-polarized GGA approach to investigate the lattice vibrations and their contribution to thermal properties of UO_2. We find that the calculated phonon dispersions are in good agreement with experimental dispersions [10] measured using inelastic neutron scattering. Computing the phonon dispersions for various lattice constants, we observed a softening of the phonon frequencies with decreasing lattice constant. Furthermore, the band gap between TA and LO modes at high-symmetry zone-boundary points are found to depend significantly on the volume. This gap almost closes at $a = 5.47$ Å, consistent with a pseudogap detected in the inelastic neutron experiment. Also, Raman and infrared active modes have been determined as a function of volume. The agreement with experimental data and with results obtained with molecular dynamics simulations is overall very good, with an exception of the infrared LO mode that appears underestimated in our first-principles calculations.

[GC2] This underestimation could possibly be improved using the GGA + U approach, which however suffers from the artifact that an improper ground state may be obtained in selfconsistent iterations. A solution to improve this artifact problem was proposed recently, the density–matrix controlling scheme which has been successfully applied to reach the ground state of UO_2 [62]. However, the density–matrix controlling scheme has not yet been tested for lattice defect calculations in a supercell and it would require further study to understand how the Hubbard U correction can be used without introducing artifacts in supercell simulations.

Including the calculated phonon contribution to the free energy, the thermal expansion coefficient and the specific heat capacity at constant pressure of UO_2 have been computed for the first time.

Both thermal quantities are found to agree well with experimental data for temperatures up to 500 K. The good correspondence of the computed and measured thermal data exemplifies the feasibility of performing first-principles modeling of the thermal properties of the important nuclear fuel material UO_2.

Acknowledgements

This work has been supported by Svensk Kärnbränslehantering AB (SKB), the Swedish Research Council (VR), the Swedish National Infrastructure for Computing (SNIC). D. L. acknowledges partial support within the framework of the 'Nanotechnology – the basis for international cooperation' – Project, Reg. No. CZ.1.07/2.3.00/20.0074 and the IT4Innovations Centre of Excellence Project, Reg. No. CZ.1.05/1.1.00/02.0070, both supported by Structural Funds of the European Union and state budget of the Czech Republic. D.L. thanks P. Pavone, University of Leoben, Leoben, Austria, and U.D. Wdowik, Pedagogical University, Cracow, Poland for fruitful discussions.

References

[1] C. Ronchi, High Temp. 45 (2007) 609.
[2] J.K. Fink, J. Nucl. Mater. 279 (2000) 1.
[3] J.J. Carbajo, G.L. Yoder, S.G. Popov, V.K. Ivanov, J. Nucl. Mater. 299 (2001) 1.
[4] K.H. Kang, K.C. Song, M.S. Yang, S.H. Lee, J.B. Ko, S.W. Kim, Int. J. Thermophys. 27 (2006) 161.
[5] Y. Yun, P.M. Oppeneer, Mater. Res. Soc. (MRS)-Bull. 36 (2011) 178.
[6] J. Bouchet, G. Jomard, J. Alloys Compd. 444–445 (2007) 271.
[7] K. Yamada, K. Kurosaki, M. Uno, S. Yamanaka, J. Alloys Compd. 307 (2000) 10.
[8] T. Watanabe, S.B. Sinnott, J.S. Tulenko, R.W. Grimes, P.K. Schelling, S.R. Phillpot, J. Nucl. Mater. 375 (2008) 388.
[9] G. Grimvall, Thermophysical Properties of Materials, enlarged and revised ed., North-Holland, Amsterdam, 1999.
[10] G. Dolling, R.A. Cowley, A.D.B. Woods, Can. J. Phys. 43 (1965) 1397.
[11] J. Schoenes, Phys. Rep. 63 (1980) 301.
[12] T. Livneh, E. Sterer, Phys. Rev. B 73 (2006) 085118.
[13] T. Livneh, J. Phys.: Condens. Mat. 20 (2008) 085202.
[14] Q. Yin, S.Y. Savrasov, Phys. Rev. Lett. 100 (2008) 225504.
[15] P. Goel, N. Choudhury, S.L. Chaplot, J. Phys.: Condens. Mat. 19 (2007) 386239.
[16] P. Goel, N. Choudhury, S.L. Chaplot, J. Nucl. Mater. 377 (2008) 438.
[17] A.J. Devey, J. Nucl. Mater. 412 (2011) 301.
[18] M. Sanati, R.C. Albers, T. Lookman, A. Saxena, Phys. Rev. B 84 (2011) 014116.
[19] S.L. Dudarev, D. Nguyen Manh, A.P. Sutton, Philos. Mag. B 75 (1997) 613.
[20] J.P. Crocombette, F. Jollet, L. Thien, T. Petit, Phys. Rev. B 64 (2001) 104107.
[21] K.N. Kudin, G.E. Scuseria, R.L. Martin, Phys. Rev. Lett. 89 (2002) 266402.
[22] R. Laskowski, G.K.H. Madsen, P. Blaha, K. Schwarz, Phys. Rev. B 69 (2004) 140408(R).
[23] I.D. Prodan, G.E. Scuseria, R.L. Martin, Phys. Rev. B 76 (2007) 033101.
[24] L.E. Roy, T. Durakiewicz, R.L. Martin, J.E. Peralta, G.E. Scuseria, C.G. Olson, J.J. Joyce, E. Guziewicz, J. Comput. Chem. 29 (2008) 2288.
[25] B. Dorado, B. Amadon, M. Freyss, M. Bertolus, Phys. Rev. B 79 (2009) 235125.
[26] B. Dorado, G. Jonard, M. Freyss, M. Bertolus, Phys. Rev. B 82 (2010) 035114.
[27] L. Petit, A. Svane, Z. Szotek, W.M. Temmerman, G.M. Stocks, Phys. Rev. B 81 (2010) 045108.
[28] Y. Yun, J. Rusz, M.-T. Suzuki, P.M. Oppeneer, Phys. Rev. B 83 (2011) 075109.
[29] R. Caciuffo, P. Santini, S. Carretta, G. Amoretti, A. Hiess, N. Magnani, L.-P. Regnault, G.H. Lander, Phys. Rev. B 84 (2011) 104409.
[30] S.L. Dudarev, G.A. Botton, S.Y. Savrasov, Z. Szotek, W.M. Temmerman, A.P. Sutton, Phys. Status Solidi 166 (1998) 429.
[31] Y. Yun, Hanchul Kim, Heemoon Lim, K. Park, Nucl. Eng. Technol. 50 (2005) 293.
[32] Y. Yun, H. Kim, H. Lim, K. Park, J. Korean Phys. Soc. 50 (2007) 1285.
[33] R. Sikora, J. Phys. Chem. Solids 66 (2005) 1069.
[34] M. Derzsi, P. Piekarz, K. Tokar, P.T. Jochym, J. Lazewski, M. Sternik, K. Parlinski, J. Phys.: Condens. Mat. 23 (2011) 105401.
[35] K. Parlinski, Z.-Q. Li, Y. Kawazoe, Phys. Rev. Lett. 78 (1997) 4063; Phys. Rev. B 61 (2000) 272.
[36] K. Parlinski, PHONON Software, Cracow, Poland, 2005.
[37] G. Kresse, J. Hafner, Phys. Rev. B 47 (1993) R558.
[38] G. Kresse, J. Furthmüller, Phys. Rev. B 54 (1996) 11169.
[39] S. Shi, X. Ke, C. Ouyang, H. Zhang, H. Ding, Y. Tang, W. Zhou, P. Li, M. Lei, W. Tang, J. Power Sour. 194 (2009) 830.
[40] S.L. Shang, L.G. Hector Jr., Y. Wang, H. Zhang, Z.K. Liu, J. Phys.: Condens. Mat. 21 (2009).
[41] P. Sindzingre, M.J. Gillan, J. Phys. C: Solid State Phys. 21 (1988) 4017.
[42] P. Zhang, B.-T. Wang, X.-G. Zhao, Phys. Rev. B 82 (2010) 144110.
[43] J.P. Perdew, Y. Wang, Phys. Rev. B 45 (1992) 13244.
[44] F. Birch, Phys. Rev. 71 (1947) 809.
[45] K. Yamada, S. Yamanaka, T. Nakagawa, M. Uno, M. Katsura, J. Nucl. Mater. 247 (1997) 289.
[46] M. Idiri, T. Le Bihan, S. Heathman, J. Rebizant, Phys. Rev. B 70 (2004) 014113.
[47] U. Benedict, G.D. Andreetti, J.M. Fournier, A. Waintal, J. Phys. (France) Lett. 43 (1982) L171.
[48] M.T. Hutchings, J. Chem. Soc., Faraday Trans. 83 (1987) 1083.
[49] G.H. Lander, J. Magn. Magn. Mater. 15 (1980) 1208.
[50] G.H. Lander, G. Aeppli, J. Magn. Magn. Mater. 100 (1991) 151.
[51] R.H. Lyddane, R.G. Sachs, E. Teller, Phys. Rev. 59 (1951) 673.
[52] R.M. Pick, M.H. Cohen, R.M. Martin, Phys. Rev. B 1 (1970) 910.
[53] J.D. Axe, G.D. Petit, Phys. Rev. 151 (1966) 676.
[54] K. Parlinski, Z.Q. Li, Y. Kawazoe, Phys. Rev. B 61 (2007) 272.
[55] D. Legut, U.D. Wdowik, J. Phys.: Condens. Mat. 22 (2010) 435402.
[56] D. Taylor, Br. Ceram. Trans. J. 83 (1984) 32.
[57] D.W. Osborne, E.F. Westrum, J. Chem. Phys. 21 (1953) 1884.
[58] J.J. Huntzicker, E.F. Westrum, J. Chem. Thermodyn. 3 (1971) 61.
[59] F. Grønvold, N.J. Kveseth, A. Sveen, J. Tichý, J. Chem. Thermodyn. 2 (1970) 665.
[60] J.K. Fink, Int. J. Thermophys. 3 (1982) 165.
[61] B. Fultz, Prog. Mater. Sci. 55 (2010) 247.
[62] B. Dorado, B. Amadon, M. Freyss, M. Bertolus, Phys. Rev. B 79 (2009) 235125.